JACS
JOURNAL OF THE AMERICAN CHEMICAL SOCIETY
Communication
pubs.acs.org/JACS

# Spin-Crossover in a Pseudo-tetrahedral Bis(formazanate) Iron Complex

Raquel Travieso-Puente,[†] J. O. P. Broekman,[†] Mu-Chieh Chang,[†] Serhiy Demeshko,[‡] Franc Meyer,[‡] and Edwin Otten*[,†]

[†]Stratingh Institute for Chemistry, University of Groningen, Nijenborgh 4, 9747 AG Groningen, The Netherlands
[‡]Institut für Anorganische Chemie, Georg-August-Universität Göttingen, Tammannstraße 4, 37077 Göttingen, Germany

Supporting Information

**ABSTRACT:** Spin-crossover in a pseudo-tetrahedral bis(formazanate) iron(II) complex (**1**) is described. Structural, magnetic, and spectroscopic analyses indicate that this compound undergoes thermal switching between an $S$=0 and an $S$=2 state, which is very rare in four-coordinate complexes. The transition to the high-spin state is accompanied by an increase in Fe−N bond lengths and a concomitant contraction of intraligand N−N bonds. The latter suggests that stabilization of the low-spin state is due to the $\pi$-acceptor properties of the ligand. One-electron reduction of **1** leads to the formation of the corresponding anion, which contains a low-spin ($S$=1/2) Fe(I) center. The findings are rationalized by electronic structure calculations using density functional theory.

Molecular compounds that show electronic bistability are of fundamental interest for the development of molecule-based data storage devices, switches, and sensors.[1] Several classes of such compounds are based on transition metal coordination complexes that can switch between low-spin (LS) and high-spin (HS) states using external stimuli such as temperature, light, or pressure. The field of spin-crossover (SCO) compounds is dominated by six-coordinate, octahedral Fe(II) complexes in which LS ($S$=0) and HS ($S$=2) states can be addressed reversibly.[2] In addition, stimulated electron transfer between a metal center and a coordinated redox-active ligand can give rise to valence tautomerism, leading to two distinct redox isomers.[3] Regardless of the electronic origin of the bistability, the overwhelming majority of molecular systems that can be switched between two spin states are based on six-coordinate, octahedral coordination compounds. Four-coordinate complexes that show changes in spin state are rare due to the decreased splitting of the d-orbitals in such compounds, with the consequence that the HS state is favored even for strong-field ligands such as cyanide.[4] In the case of iron complexes, exceptions to this are the three-fold symmetric, four-coordinate phosphinimido complexes with a tris(carbene)borate ligand reported by Smith et al.,[5] and the square-planar (bis)-iminopyridine iron imidos of Chirik et al.[6]

Here we report a pseudo-tetrahedral bis(formazanate) iron complex that shows SCO. Spectroscopic, crystallographic, and magnetic data are consistent with the complex being in a LS ($S$=0) state at low temperature and converting to a HS ($S$=2) state upon heating. The role of the formazanate ligands, which have recently attracted attention as redox-active $\beta$-diketiminate analogues,[7−9] in mediating this chemistry is explored.

**Scheme 1**

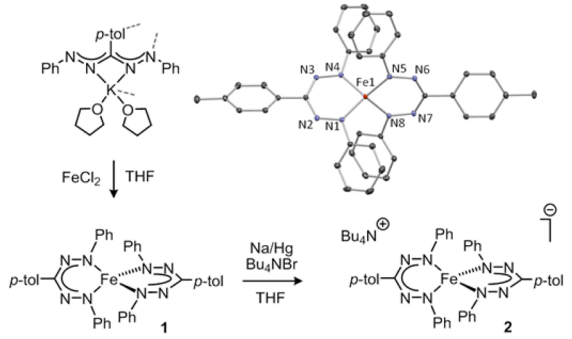


Treatment of $FeCl_2$ with 2 equiv of the formazanate salt K[PhNNC($p$-tol)NNPh]·2THF (prepared as previously reported)[10] in THF provided the desired bis(formazanate) iron complex (PhNNC($p$-tol)NNPh)$_2$Fe (**1**) (Scheme 1). Extraction of the product into toluene and crystallization from a toluene/hexane mixture afforded **1** in 63% yield as dark red crystals. $^1$H NMR spectroscopy in $C_6D_6$ at room temperature showed the expected number of resonances for equivalent, symmetric formazanate ligands. The signals are found in the normal diamagnetic range (between $\delta$ 12 and −1 ppm), but all show broadening. 2D NMR spectroscopy facilitated the full assignment of the $^1$H and $^{13}$C NMR spectra and indicated several of the signals to be paramagnetically shifted. Variable-temperature $^1$H NMR in toluene-$d_8$ revealed substantial changes to the spectrum upon cooling, with all resonances approaching their expected diamagnetic values at 215 K (Figure S1). Conversely, at 385 K the signals are spread between $\delta$ 20 and −10 ppm. These data indicate a temperature-dependent spin equilibrium with a diamagnetic ($S$=0) ground state at low temperature. The $^1$H chemical shift dependence was fitted using the ideal solution model equation[5b,11] (Figure 1; see Supporting Information (SI) for details) to afford the thermodynamic data for the spin equilibrium as $\Delta H$ = 22.2(3) kJ/mol and $\Delta S$ = 64(1) J/(mol K), which indicates a SCO temperature $T_{1/2}$ = 345 K. These thermodynamic values are similar to those found in Smith's four-coordinate Fe(II) complexes,[5] as well as many six-coordinate

**Received:** February 11, 2016
**Published:** April 14, 2016




DOI: 10.1021/jacs.6b01552
J. Am. Chem. Soc. 2016, 138, 5503−5506

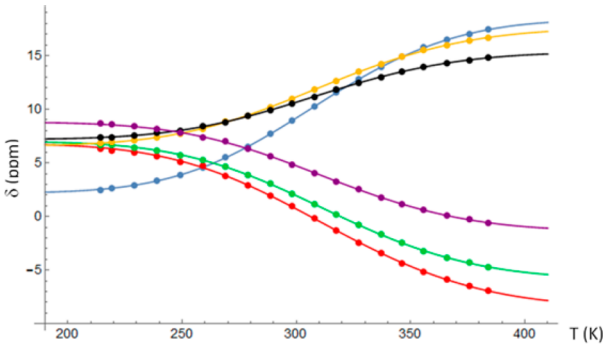


**Figure 1.** Temperature dependence of the $^1$H NMR signals of **1** (toluene-$d_8$ solution). Data fitted with the ideal solution model equation; see text for details.

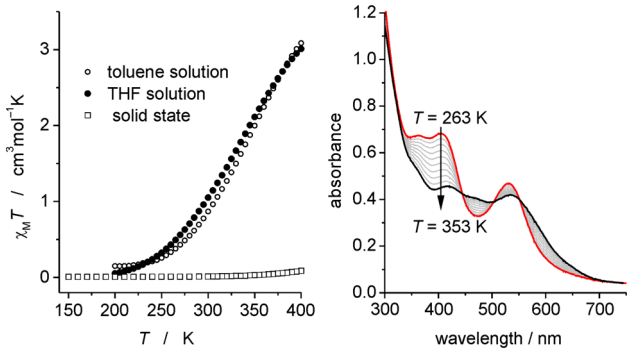


**Figure 2.** Left: magnetic susceptibility measurements for **1** in the solid state and in solution (THF and toluene). Right: variable-temperature UV/vis spectra for **1** in toluene in the range 263−353 K.

Fe(II) SCO compounds.[12] The solution magnetic moment (Evans method in THF-$d_8$) was measured between 260 and 340 K, and found to vary between 1.9 and 3.7 $\mu_B$ (or 0.46 and 1.74 $cm^3 \cdot mol^{-1} \cdot K$). The values are consistent with an incomplete transition to a HS ($S$=2) complex.

The LS ($S$=0) state of **1** is unusual, since $d^6$ metals with four-coordinate geometries adopt either $S$=1 (square planar) or $S$=2 (tetrahedral) ground states.[4b,13] The only exceptions are planar bis(imino)pyridine iron imides reported by Chirik,[6] and $C_{3v}$-symmetric compounds based on tripodal ligands: an anionic Fe(II) imido by Peters et al.,[14] and neutral Fe(II) phosphinimido complexes reported by Smith et al.[5] In the latter compounds, the LS state is favored due to substantial destabilization of the $d_{xz}$/$d_{yz}$-orbitals which have Fe−N $\pi$*-character, whereas the $d_{z^2}$-orbital is anomalously low in energy and essentially nonbonding in an axially distorted ($C_{3v}$) geometry.[15] The distinct differences in coordination geometry and ligand set in these compounds and those in **1** prompted a more detailed analysis of **1** by magnetic, spectroscopic, and computational studies.

Single-crystal X-ray diffraction at 100 K showed that **1** adopts a flattened, pseudo-tetrahedral coordination geometry with two bidentate formazanate ligands bound through the terminal N atoms (Scheme 1). The Fe center is located in the planes of the formazanate ligands and features Fe−N bond distances in the range of 1.8174(16)−1.8330(16) Å. These are shorter than those found in structurally related HS-Fe(II) complexes with bidentate ligands (e.g., $\beta$-diketiminate,[16] $\beta$-ketoiminate,[17] amidinate,[18] or 1,3,5-triazapentadienyl[19]), which have Fe−N distances of >2.0 Å. This discrepancy is consistent with a difference in spin state compared to **1**: in the LS complex **1**, the d-orbitals that are metal−ligand antibonding are unoccupied. In addition, the N−N bonds in the ligand backbone are elongated (1.327(2)−1.329(2) Å) in comparison to the bond lengths normally observed in formazanate complexes (1.30−1.31 Å).[7b,8] The temperature dependence of the spin state observed by $^1$H NMR spectroscopy prompted collection of an X-ray diffraction data set at elevated temperature. The structure of **1** remains invariant up to 400 K, but at 450 K a transition to a different monoclinic unit cell is observed with a 7% increase in volume. The Fe−N bond lengths are elongated to 1.909(4)−1.920(4) Å, whereas the N−N bonds are shortened (1.303(5)−1.319(5) Å) on going from 100 to 450 K (see Table S2 for a comparison of metrical parameters). The coordination geometry at 450 K more closely resembles that of a tetrahedron, with an angle between the ligand coordination planes N(1)−Fe(1)−N(4)/N(5)−Fe(1)−N(8) of 77.80° (cf. 60.97° at 100 K).

Magnetic susceptibility measurements for **1**, recorded on a SQUID magnetometer both in the solid state and in solution (THF and toluene), confirm its diamagnetic nature at low temperatures (Figure 2). The $\chi_M T$ product in the solid state is almost temperature-independent between 2 and 400 K, indicating that in the solid state **1** remains LS up to 400 K.

In agreement with the X-ray crystallography results, these data indicate that, in the solid state, the spin transition is abrupt and takes place somewhere between 400 and 450 K. This is further confirmed by differential scanning calorimetry analysis of solid **1**, which shows a sharp endothermic transition at 428 K. Conversely, the solution magnetization starts to increase at 200 K, and at 400 K (the highest temperature accessible) it reaches $\chi_M T \approx 3$ $cm^3 \cdot K \cdot mol^{-1}$. Although the spin transition is incomplete at that temperature, the data are consistent with an $S$=2 ground state with some degree of orbital contribution to the magnetic moment. UV/vis spectroscopy at room temperature shows a strong absorbance in the visible region ($\lambda_{max}$ = 532 nm, $\varepsilon$ = 11 900 $M^{-1} \cdot cm^{-1}$), which is typical for electronic transitions localized within the formazanate ligand framework.[7b,8a,9c,20] Variable-temperature UV/vis measurements of **1** in toluene show prominent spectral changes reflecting the SCO (Figure 2). Quantitative modeling of the absorbance intensities assuming Boltzmann behavior of the spin equilibrium yields thermodynamic parameters in excellent agreement with NMR results and reveals that the mole fraction of the HS state in toluene changes from ∼0.12 at 263 K to 0.63 at 353 K (see SI for details).

The electronic structure of **1** was probed further by zero-field $^{57}$Fe Mössbauer spectroscopy at 80 and 300 K in the solid state (Figures 3 and S6). A quadrupole doublet was observed with isomer shift $\delta$ = 0.03 mm/s and quadrupole splitting $\Delta E_Q$ = 2.05 mm/s at 80 K, which is shifted to $\delta$ = −0.05 mm/s ($\Delta E_Q$ = 1.96 mm/s) at 300 K due to the second-order Doppler effect.[21]

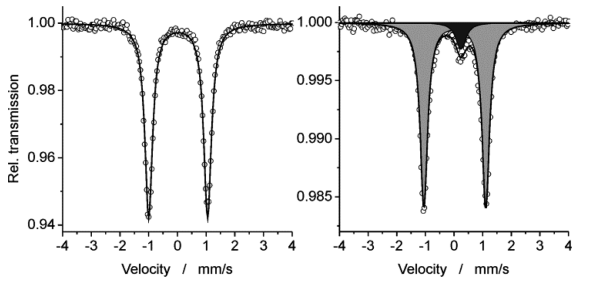


**Figure 3.** Mössbauer spectra of **1** at 80 K in the solid state (left) and in frozen THF solution (right).



DOI: 10.1021/jacs.6b01552
J. Am. Chem. Soc. 2016, 138, 5503−5506

Spectra similar to the spectrum observed in the solid state were obtained in THF and in toluene solutions ($\delta$ = 0.03 mm/s; $\Delta E_Q$ = 2.16 mm/s at 80 K in THF); however, an additional absorption with a higher isomer shift ($\delta$ = 0.24 mm/s; $\Delta E_Q$ = 0.09 mm/s) accounting for ~9% of unknown impurity was observed (Figure 3). These isomer shifts are typical for LS-Fe(II) complexes (typically between −0.3 and 0.4 mm/s), whereas HS-Fe(II) complexes exhibit characteristic isomer shifts of 0.7−1.4 mm/s.[22]

Cyclic voltammetry of **1** in THF (0.1 M $Bu_4NPF_6$) shows two (quasi)reversible redox waves at $E^0$ = −1.21 and −2.01 V, and an irreversible redox wave at ~ +0.27 V (all potentials vs $Fc^{0/+}$, Figure S15). The redox wave at +0.27 V is assigned to the $Fe^{II/III}$ redox couple.[17] The redox wave at −1.21 V is less readily assigned: both an $Fe^{I/II}$ redox couple and a ligand-based reduction[8] could occur in that range. A comparison to the zinc analogue of **1**, in which successive one-electron reductions of the ligand occur within 0.3 V of each other (−1.39/−1.68 V),[8] indicates that **1** behaves differently and suggests a metal-based reduction (*vide infra*). Chemical synthesis of the one-electron-reduced compound $[Bu_4N][(PhNNC(p\text{-tol})NNPh)_2Fe]$ (**2**) was accomplished in 90% yield by treatment of **1** with 1 equiv of Na/Hg in the presence of $Bu_4NBr$. Both solution (Evans method) and solid-state (SQUID, Figure S7) magnetic measurements indicate a rare $S$=1/2 spin ground state[23] for **2** at all temperatures examined (solution data measured between 220 and 360 K in THF-$d_8$). X-ray analysis at 100 K shows a (flattened) pseudo-tetrahedral coordination geometry around the Fe center in **2** (Figure S5) similar to that of LS **1**, with Fe−N bond lengths (1.8562(19)/1.8755(19) Å) that are elongated relative to those in the 100 K structure of **1**. Compound **2** has N−N bonds within the ligand chelates of 1.344(3) and 1.347(3) Å, somewhat longer than in **1**, and the angle between the ligand coordination planes is similar (62.62°). The Mössbauer spectrum of **2** shows an (asymmetric) quadrupole doublet at $\delta$ = 0.22 mm/s and $\Delta E_Q$ = 2.58 mm/s at 80 K, which remains unchanged between 12 and 140 K (Figure 4). The asymmetric line broadening due to slow relaxation processes is typical for compounds with odd numbers of unpaired electrons.[24] The increase in the isomer shift, which is typically observed upon reduction, is taken as an indication that **2** contains a LS-Fe(I) center, and is in line with reported isomer shifts of 0.2−0.4 mm/s for LS-Fe(I).[22] An EPR signal at $g$ = 2.05 was observed in THF at room temperature, which changes to a rhombic signal upon cooling to 77 K, with $g_1$ = 2.15, $g_2$ = 2.04, and $g_3$ = 1.97 (Figure 4). These values are consistent with an $S$=1/2 system with significant spin−orbit coupling and therefore a SOMO with Fe d-character.

To shed light on the origin of the unusual $S$=0 spin state observed for **1**, DFT calculations at the B3LYP/TZVP level using X-ray coordinates were initially evaluated using the ORCA

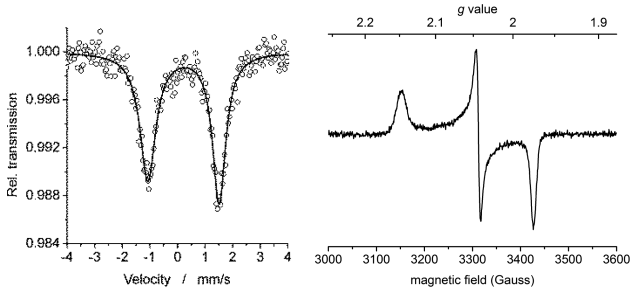


**Figure 4.** Mössbauer (solid state, 80 K, left) and X-band EPR (in THF, 77 K, right) spectra of **2**.

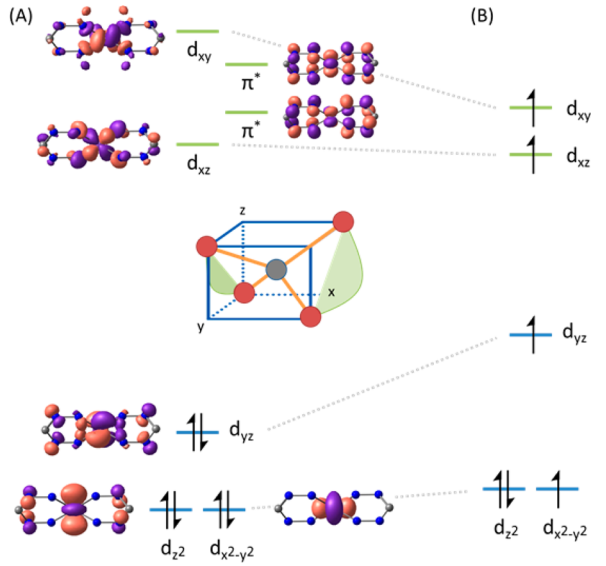


**Figure 5.** Molecular orbital diagram for **1** in the LS ($S$=0) state (A) and the HS ($S$=2) state (B). Orbitals shown are obtained from a restricted closed-shell DFT calculation (atoms other than those in the ligand backbone are omitted for clarity).

program[25] to estimate the relative energies of various spin states of **1**. From these calculations it appeared that the energies of singlet (either open- (broken-symmetry) or closed-shell) and triplet states were within 3 kcal/mol of each other, whereas the quintet was significantly higher in energy (24 kcal/mol). Geometry optimizations at this level of theory (using Gaussian 09)[26] indicated a HS ($S$=2) ground state, as may be anticipated for the hybrid functional B3LYP.[27] For all calculated spin states, the Fe−N distances are elongated (>1.857 Å) compared to those observed by crystallography. In addition, the N−N distances are predicted to be shorter (<1.303 Å) than observed experimentally. These discrepancies suggested that B3LYP does not provide an accurate description of **1**. Testing a range of functionals (with the TZVP basis set, see SI) resulted in the best agreement with the experimental geometry for the pure functional BP86, with a closed-shell singlet state lowest in energy. The calculated Mössbauer isomer shift at that geometry (using an enlarged CP(PPP) basis set for Fe)[28] agrees well with experiment ($\delta$ = 0.03 mm/s), whereas the quadrupole splitting is underestimated ($\Delta E_Q$ = −1.63 mm/s). Higher spin states give larger calculated isomer shifts ($\delta$ > 0.3 mm/s) that are inconsistent with experimental data. Analysis of the Kohn−Sham orbitals at the BP86/TZVP-optimized geometry shows that the bidentate formazanate ligands interact with the metal d-orbitals to give the orbital energy diagram shown in Figure 5A. The ligands engage in $\pi$-backbonding with the Fe $d_{yz}$-orbital, which as a consequence is significantly stabilized relative to the $d_{xz}/d_{xy}$-orbitals. The short Fe−N and long N−N bond distances observed experimentally are ascribed to this $\pi$-backbonding interaction. An alternative description of the electronic structure, in which a LS-Fe(III) ($S$=1/2) center is anti-ferromagnetically coupled to a ligand-based radical, would also account for the anomalous structural and magnetic features of **1** (valence tautomerism).[3] However, the calculations provide little evidence that this description is accurate: the magnetic orbitals for the broken-symmetry solutions are predominantly metal-based; thus, the formazanates in **1** behave as $\pi$-acceptors rather than "redox-active" ligands.[6,29] Calculations for the experimentally


DOI: 10.1021/jacs.6b01552
J. Am. Chem. Soc. 2016, 138, 5503−5506

observed HS state indicate that this is best described as containing a conventional $S$=2 Fe(II) center.

Similar BP86/TZVP calculations on the anionic moiety in **2** indicate an $S$=1/2 ground state, with the unpaired electron in a d-orbital. Attempts to converge on a broken-symmetry solution were not successful. The computed Mössbauer parameters ($\delta$ = 0.17 mm/s; $\Delta E_Q$ = −1.82 mm/s) and $g$-tensor (2.15, 2.11, 2.02) at the DFT-optimized geometry are in good agreement with the empirical data and validate the electronic structure description obtained from these DFT calculations.

The structural, magnetic, and spectroscopic data presented here firmly establish rare low-spin ground states for **1** ($S$=0) and **2** ($S$=1/2). Notably, the reason for this is quite different from that found in the LS four-coordinate complexes reported to date, in which an axial ("umbrella") distortion combined with a strong $\pi$-donor ligand causes a large d-orbital energy gap.[4b,30] In **1** and **2** these features are absent; instead, the stabilization of the LS state is due to the $\pi$-acceptor properties of the anionic formazanate ligands. Overall, this provides a new design strategy for spin-crossover compounds. It is anticipated that the SCO properties of **1** can be modified by changing the steric/electronic characteristics of the formazanate ligands. In addition, investigation of the reactivity of **1**, **2**, and related low-coordinate complexes toward various small-molecule substrates is anticipated to lead to new insight in the spin-state dependence of reaction pathways.

## ■ ASSOCIATED CONTENT

### Supporting Information

The Supporting Information is available free of charge on the ACS Publications website at DOI: 10.1021/jacs.6b01552.

Experimental procedures; details of spectroscopic and magnetic characterization; computational studies (PDF)
Crystallographic data for **1** and **2** (CIF)

## ■ AUTHOR INFORMATION


### Corresponding Author

*edwin.otten@rug.nl


### Notes

The authors declare no competing financial interest.

## ■ ACKNOWLEDGMENTS

Financial support from The Netherlands Organization for Scientific Research (NWO) is gratefully acknowledged (Veni grant to E.O.). We thank COST Action CM1305 for supporting a short-term scientific mission (STSM-CM1305-021115-067634 to R.T.-P.) to measure SQUID/Mössbauer data in Göttingen. We thank Dr. Remco Havenith for useful discussions regarding the DFT calculations.

## ■ REFERENCES


(1) (a) Létard, J.-F.; Guionneau, P.; Goux-Capes, L. In *Spin Crossover in Transition Metal Compounds III*; Springer: Berlin, 2004; Vol. *235*, p 221. (b) Sato, O.; Tao, J.; Zhang, Y.-Z. *Angew. Chem., Int. Ed.* **2007**, *46*, 2152.

(2) Halcrow, M. A. *Spin-Crossover Materials: Properties and Applications*; John Wiley & Sons: Somerset, NJ, 2013.

(3) (a) Hendrickson, D. N.; Pierpont, C. G. In *Spin Crossover in Transition Metal Compounds II*; Springer: Berlin, 2004; Vol. *234*, p 63. (b) Boskovic, C. In *Spin-Crossover Materials*; John Wiley & Sons: Somerset, NJ, 2013; p 203. (c) Tezgerevska, T.; Alley, K. G.; Boskovic, C. *Coord. Chem. Rev.* **2014**, *268*, 23.

(4) (a) Buschmann, W. E.; Arif, A. M.; Miller, J. S. *Angew. Chem., Int. Ed.* **1998**, *37*, 781. (b) Alvarez, S.; Cirera, J. *Angew. Chem., Int. Ed.* **2006**, *45*, 3012.

(5) (a) Scepaniak, J. J.; Harris, T. D.; Vogel, C. S.; Sutter, J.; Meyer, K.; Smith, J. M. *J. Am. Chem. Soc.* **2011**, *133*, 3824. (b) Lin, H.-J.; Siretanu, D.; Dickie, D. A.; Subedi, D.; Scepaniak, J. J.; Mitcov, D.; Clérac, R.; Smith, J. M. *J. Am. Chem. Soc.* **2014**, *136*, 13326.

(6) Bowman, A. C.; Milsmann, C.; Bill, E.; Turner, Z. R.; Lobkovsky, E.; DeBeer, S.; Wieghardt, K.; Chirik, P. J. *J. Am. Chem. Soc.* **2011**, *133*, 17353.

(7) (a) Gilroy, J. B.; Ferguson, M. J.; McDonald, R.; Patrick, B. O.; Hicks, R. G. *Chem. Commun.* **2007**, 126. (b) Chang, M. C.; Otten, E. *Chem. Commun.* **2014**, *50*, 7431.

(8) (a) Chang, M.-C.; Dann, T.; Day, D. P.; Lutz, M.; Wildgoose, G. G.; Otten, E. *Angew. Chem., Int. Ed.* **2014**, *53*, 4118. (b) Chang, M.-C.; Roewen, P.; Travieso-Puente, R.; Lutz, M.; Otten, E. *Inorg. Chem.* **2015**, *54*, 379.

(9) (a) Protasenko, N. A.; Poddel'sky, A. I.; Bogomyakov, A. S.; Fukin, G. K.; Cherkasov, V. K. *Inorg. Chem.* **2015**, *54*, 6078. (b) Mandal, A.; Schwederski, B.; Fiedler, J.; Kaim, W.; Lahiri, G. K. *Inorg. Chem.* **2015**, *54*, 8126. (c) Schorn, W.; Grosse-Hagenbrock, D.; Oelkers, B.; Sundermeyer, J. *Dalton Trans.* **2016**, *45*, 1201. (d) Kabir, E.; Wu, C.-H.; Wu, J. I. C.; Teets, T. S. *Inorg. Chem.* **2016**, *55*, 956.

(10) Travieso-Puente, R.; Chang, M.-C.; Otten, E. *Dalton Trans.* **2014**, *43*, 18035.

(11) Kläui, W.; Eberspach, W.; Gütlich, P. *Inorg. Chem.* **1987**, *26*, 3977.

(12) Gütlich, P.; Hauser, A.; Spiering, H. *Angew. Chem., Int. Ed. Engl.* **1994**, *33*, 2024.

(13) (a) Poli, R. *Chem. Rev.* **1996**, *96*, 2135. (b) Cirera, J.; Ruiz, E.; Alvarez, S. *Inorg. Chem.* **2008**, *47*, 2871.

(14) Brown, S. D.; Peters, J. C. *J. Am. Chem. Soc.* **2005**, *127*, 1913.

(15) (a) Jenkins, D. M.; Di Bilio, A. J.; Allen, M. J.; Betley, T. A.; Peters, J. C. *J. Am. Chem. Soc.* **2002**, *124*, 15336. (b) Tangen, E.; Conradie, J.; Ghosh, A. *J. Chem. Theory Comput.* **2007**, *3*, 448.

(16) (a) Morris, W. D.; Wolczanski, P. T.; Sutter, J.; Meyer, K.; Cundari, T. R.; Lobkovsky, E. B. *Inorg. Chem.* **2014**, *53*, 7467. (b) Panda, A.; Stender, M.; Wright, R. J.; Olmstead, M. M.; Klavins, P.; Power, P. P. *Inorg. Chem.* **2002**, *41*, 3909.

(17) Granum, D. M.; Riedel, P. J.; Crawford, J. A.; Mahle, T. K.; Wyss, C. M.; Begej, A. K.; Arulsamy, N.; Pierce, B. S.; Mehn, M. P. *Dalton Trans.* **2011**, *40*, 5881.

(18) (a) Hagadorn, J. R.; Arnold, J. *Inorg. Chem.* **1997**, *36*, 132. (b) Vendemiati, B.; Prini, G.; Meetsma, A.; Hessen, B.; Teuben, J. H.; Traverso, O. *Eur. J. Inorg. Chem.* **2001**, 707. (c) Nijhuis, C. A.; Jellema, E.; Sciarone, T. J. J.; Meetsma, A.; Budzelaar, P. H. M.; Hessen, B. *Eur. J. Inorg. Chem.* **2005**, 2089. (d) Zhang, L.; Xiang, L.; Yu, Y.; Deng, L. *Inorg. Chem.* **2013**, *52*, 5906.

(19) Liu, F.; Qiao, X.; Wang, M.; Zhou, M.; Tong, H.; Guo, D.; Liu, D. *Polyhedron* **2013**, *52*, 639.

(20) Barbon, S. M.; Price, J. T.; Reinkeluers, P. A.; Gilroy, J. B. *Inorg. Chem.* **2014**, *53*, 10585.

(21) Unfortunately, temperatures above 300 K were not accessible, and the HS state could not be observed by Mössbauer spectroscopy.

(22) Gütlich, P. *Z. Anorg. Allg. Chem.* **2012**, *638*, 15.

(23) (a) Mankad, N. P.; Whited, M. T.; Peters, J. C. *Angew. Chem., Int. Ed.* **2007**, *46*, 5768. (b) Lee, Y.; Kinney, R. A.; Hoffman, B. M.; Peters, J. C. *J. Am. Chem. Soc.* **2011**, *133*, 16366. (c) Anderson, J. S.; Peters, J. C. *Angew. Chem., Int. Ed.* **2014**, *53*, 5978. (d) Hickey, A. K.; Chen, C.-H.; Pink, M.; Smith, J. M. *Organometallics* **2015**, *34*, 4560.

(24) Gütlich, P.; Bill, E.; Trautwein, A. X. *Mössbauer spectroscopy and transition metal chemistry*; Springer: Heidelberg, 2011.

(25) Neese, F. *WIREs Comput. Mol. Sci.* **2012**, *2*, 73.

(26) Frisch, M. J.; et al. *Gaussian 09*, Revision D.01; Gaussian, Inc.: Wallingford, CT, 2009.

(27) (a) Ye, S.; Neese, F. *Inorg. Chem.* **2010**, *49*, 772. (b) Kepp, K. P. *Coord. Chem. Rev.* **2013**, *257*, 196.

(28) Römelt, M.; Ye, S.; Neese, F. *Inorg. Chem.* **2009**, *48*, 784.

(29) Chirik, P. J. *Inorg. Chem.* **2011**, *50*, 9737.

(30) Cirera, J.; Ruiz, E. *Inorg. Chem.* **2016**, *55*, 1657.




DOI: 10.1021/jacs.6b01552
J. Am. Chem. Soc. 2016, 138, 5503−5506